In this chapter the major features of the shielding of electrons and photons at accelerators are described. It includes extensive discussion of the electromagnetic cascade and a discussion of the shielding of photoneutrons and high energy particles that result from these interactions. The chapter concludes with a treatment of the generalized shielding problem with specific attention given to the Monte-Carlo method and with a brief summary of magnetic deflections of charged particles which are of general applicability to radiation protection at particle accelerators.

I. The Electromagnetic Cascade-Introduction

The major feature that needs to be considered in the shielding design at electron accelerators is the electromagnetic cascade. One should recall the definitions of **critical energy**, E_c and **radiation length**, X_o, that were given in Eq. (1.20) and (1.22). Another parameter of importance for describing the electromagnetic cascade is the **Molière radius**, X_m:

$$X_m = X_o E_s / E_c \tag{2.1}$$

$$\text{where} \quad E_s = (\sqrt{4\pi / \alpha}) m_e c^2 = 21.2\,MeV\,, \tag{2.2}$$

where α is the fine structure constant (see Table 1.1), and m_e is the mass of the electron. X_m is a good characteristic length for describing radial distributions in electromagnetic showers. Two more dimensionless scaling variables are commonly introduced to describe electromagnetic shower behavior;

$$t = x/X_o \quad \text{(distance)} \tag{2.3}$$

$$\text{and} \quad y = E/E_c \quad \text{(energy)}. \tag{2.4}$$

For mixtures of n elements these quantities and the stopping power dE/dx scale according to the elemental fractions by weight, f_i, as follows, according to the Particle Data Group (PDG96):

$$\frac{dE}{dx} = \sum_{i=1}^{n} f_i \left(\frac{dE}{dx}\right)_i \tag{2.5}$$

where all stopping powers are expressed as energy loss per unit areal density (e.g., MeV $cm^2\ g^{-1}$). For convenience, as defined in Chapter 1,

$$E_c = 800/(Z + 1.2) \ \text{(MeV)}, \tag{2.6}$$

$$\text{and} \quad X_0 = \frac{716.4A}{Z(Z+1)\ln(287/\sqrt{Z})} \ \ (\text{g cm}^{-2}). \tag{2.7}$$

Another term employed is that of the so-called **Compton minimum** which, as the term is generally used, is the energy at which the total photon cross section is at a minimum and the **photon mean free path**, λ_γ, is thus, a maximum. The use of this term is somewhat inaccurate since at the higher energies the Compton scattering cross section *monotonically* decreases with energy. This value always occurs at energies less than E_c and is typically a few MeV. Figures 2.1 and 2.2 give values of the photon mean free path for a variety of materials.

For high energy photons (E_o > 1 GeV), the total e^+e^- pair production cross section, σ_{pair}, is approximately given, for a single element, by

$$\sigma_{pair} = \frac{7}{9}\left(\frac{A}{X_0 N_A}\right) \quad (\text{cm}^2), \tag{2.8}$$

where A is the atomic weight, N_A, is Avagadro's number, and X_o is the radiation length expressed in units of g/cm^2. For energies larger than a few MeV, the pair production process dominates the total photon attenuation. The interaction length for pair production, λ_{pair}, is thus given by

$$\lambda_{pair} = \frac{\rho}{N\sigma}(\text{g cm}^2) = \frac{\rho}{\frac{\rho N_A}{A}\frac{7}{9}\left(\frac{A}{X_0 N_A}\right)} = \frac{9}{7}X_0, \tag{2.9}$$

where the symbols all have the same meanings as used previously. This result, along with the facts about photon production by electrons interacting in matter, leads to the most important fact about the electromagnetic cascade:

> **The electrons radiatively produce photons with almost the same characteristic length for which the photons produce more e^+ e^- pairs.**

This is so important because as a first order approximation it means that the "size" in physical space is independent of energy. For hadronic cascades, we will see that the result is considerably different.

Before discussing further the electronmagnetic cascade process in detail, one must look a bit more at the dose equivalent due to thick-target bremsstrahlung dose at large values of θ for targets surrounded by cylindrical shields. This has been done by Swanson and Thomas (Sw90) with improvements suggested by Nelson (Ne97). A picture of the situation is given in Fig. 2.3. Without including the attenuation by shielding, the normalized differential yield, $dN/d\Omega$, per incident electron of photons of all energies is given by:

$$\frac{1}{E_o}\frac{dN}{d\Omega} = 4.76E_o\exp(-\theta^{0.6}) + 1.08\exp(\theta/72) \text{ (photons sr}^{-1}\text{ GeV}^{-1}\text{ electron}^{-1}), \tag{2.10}$$

while the absorbed dose per incident electron, D, external to shielding is described by,

$$D(\theta) = (1\times 10^{-15})\left\{10.2E_o \exp(-\theta^{0.6}) + 2.3\exp(\theta/72)\right\}E_o\left(\frac{\sin\theta}{a+d}\right)^2 \exp\left(-\frac{\mu}{\rho}\frac{\rho d}{\sin\theta}\right)$$

(Gy/electron). (2.11)

These expressions are based on results involving iron and copper targets at E_0 = 15 GeV. In these equations, E_0 is in GeV, θ is in degrees, a is the target-to-shield distance (meters), d is the shield thickness (meters), ρ is the shielding material density (kg m^{-3}), and μ/ρ is the attenuation coefficient equal to the value at the "Compton minimum" which for concrete is 2.4 x 10^{-3} m^2kg^{-1}. The formulae implicitly assume a dose equivalent per unit fluence appropriate at the shower maximum. For conditions of no shielding present (d = 0), the values are within factors of 2 to 5 of those obtained using Eq. (1.25-1.27). Armed with this useful parameterization, we shall now proceed to further discussion of the details of development of the electromagnetic cascade.

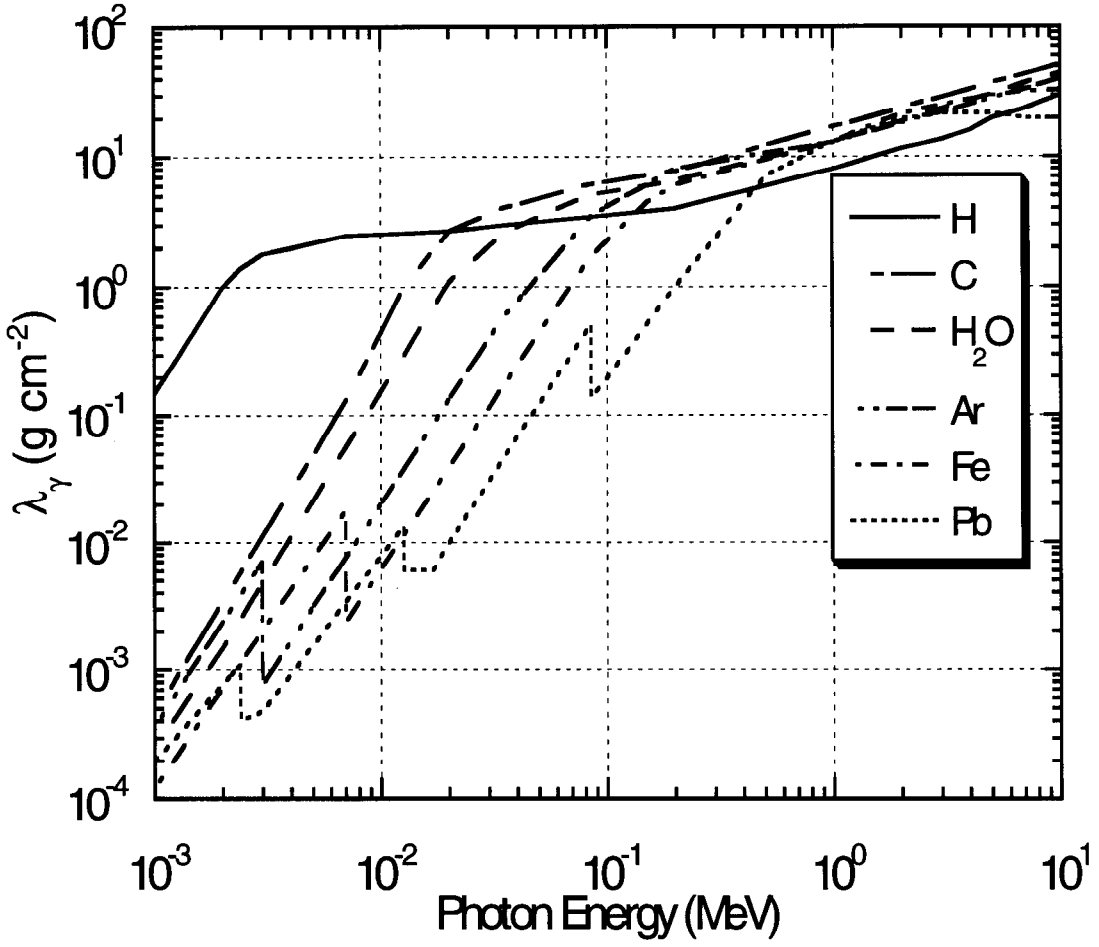

Fig. 2.1 Photon mean free path as a function of photon energy in various materials for low energies. [Adapted from (PDG96).]

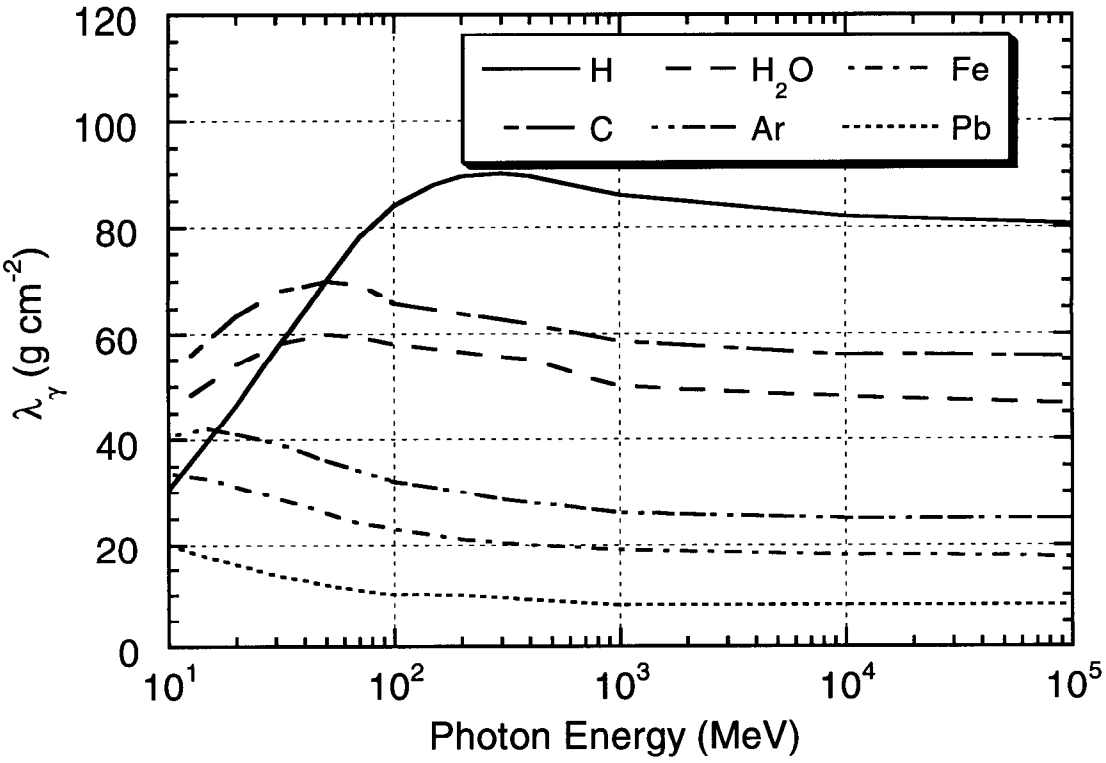

Fig. 2.2 Photon mean free path as a function of photon energy in various materials for high energies. [Adapted from (PDG96).]

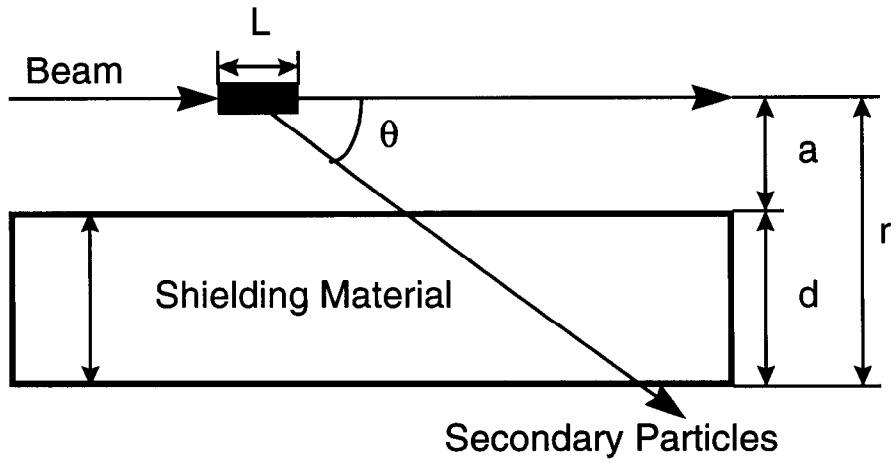

Fig. 2.3 Target and shielding geometry for the estimation of dose equivalent due to electron beam interactions with a target surrounded by shielding. *L* is the length of the target and the other parameters specify the geometry.

II. The Electromagnetic Cascade Process

In the most simple terms, the electromagnetic cascade at an electron accelerator proceeds qualitatively according to the following steps:

1. A high energy electron (Eo >> $m_e c^2$) produces a high energy photon by bremsstrahlung.

2. This photon produces an e^+ e^- pair after traveling, on average, a distance of X_o. Each member of the pair will have, on average, half the energy of the photon.

3. After traveling an average distance of X_o, each member of the e^+ e^- pair will produce yet another bremsstrahlung photon.

4. Each electron or positron may continue on to interact again and release yet more photons before its energy is totally absorbed.

This chain of events can equally well be initiated by a high energy photon, even one produced in secondary interactions at a hadron accelerator. Eventually, after a number of generations, the individual energies of the electrons and positrons will be degraded to values below E_c so that ionization processes then begin to dominate and terminate the shower. Likewise, the photon energies eventually are degraded so that Compton scattering and the photoelectric effect compete with the further production of e^+ e^- pairs. Figure 2.4 schematically shows the basic electromagnetic cascade process.

Of course, there are subtleties representing many different physical processes, such as the production of other particles, which must be taken into account and are best handled by Monte-Carlo calculations. The most widely-used code incorporating the Monte-Carlo method applied to electromagnetic cascades is EGS (electron gamma shower) which was written by W. R. Nelson and described by Nelson et al. (Ne90).[1] A. Van Ginneken has also written a Monte-Carlo program called AEGIS (Va78) which is very effective for calculating the propagation of such cascades through thick shields. At the end of this Chapter, the Monte-Carlo Method will be reviewed. Analytical approximations have been developed and are summarized elsewhere [e.g., (Sw79)]. The results of published calculations are used in the following discussion to aid in improving the reader's understanding of electromagnetic cascades.

Longitudinal shower development

The dosimetric properties of the calculations of an electromagnetic cascade may be summarized in curves that give fluence, dose, or other quantities of interest as functions of shower depth or distance from the axis. Figure 2.5 shows the fraction of total energy

[1]Monte-Carlo programs exist, in general, in a state of nearly continuous improvement. Thus the authors of such codes should be contacted to provide the current version.

deposited (integrated over all radii about the shower axis) versus depth from Van Ginneken and Awschalom (Va75). These authors identified a scaling parameter, ζ, given by:

$$\zeta = 325(\ln Z)^{-1.73}\ln E_0 \quad (\text{g cm}^{-2}), \tag{2.12}$$

where E_o is in MeV. When longitudinal coordinates are expressed in units of ζ,, all curves merge approximately into this universal one and are rather independent of target material.

Rossi and Griesen (Ro41), in their development of analytical shower theory, have predicted, using their so-called "Approximation B", that the total number of electrons and positrons at the shower maximum, N_{show} are proportional to the primary energy as follows for an electron-initiated shower:

$$N_{show} = \frac{0.31 E_0/E_c}{\sqrt{\ln(E_0/E_c) - 0.37}}. \tag{2.13}$$

This is intuitively sensible as the final outcome of the shower is to divide the energy at maximum among a number of particles with energies near E_c. For a photon-initiated shower, the constant of 0.37 in the denominator becomes 0.18. One can obtain the maximum energy deposited per radiation length from Eq. (2.13) as the product $E_c N_{show}$ (Sc90).

Also from Approximation B, the location of the shower maximum X_{max}, (along the longitudinal axis usually represented by the z-coordinate) should be given by:

$$\frac{X_{\max}}{X_o} = \ln\left(\frac{E_o}{E_c}\right) - C, \qquad \text{with C = 1.} \tag{2.14}$$

Experimentally, Bathow, et al. (Ba67) found that values of $C = 0.77$ for Cu and $C = 0.47$ for Pb fit data better. Also, photon-induced showers penetrate about 0.8 radiation lengths deeper. Schopper et al. (Sc90) simply give values of $C = 1$ and $C = 0.5$ for electron- and photon-initiated showers, respectively.

There are slight differences between photon and electron-induced showers but these can normally be neglected. The maximum energy deposited per radiation length is simply given by multiplying N_{show} by the critical energy, E_c. Schopper et al (Sc90) gives the mean squared *longitudinal* spread, τ^2, (mean square distance lateral spread of the shower about $t \approx t_{max} = X_{max}/X_o$.):

$$\tau^2 = 1.61 \ln\left(\frac{E_o}{E_c}\right) - 0.2 \qquad \text{(electron-induced shower), and} \tag{2.15}$$

$$\tau^2 = 1.61 \ln\left(\frac{E_o}{E_c}\right) + 0.9 \qquad \text{(photon-induced shower).} \tag{2.16}$$

EGS4 results tabulated by Schopper et al. (Sc90) have been parameterized to determine "source terms", S_i, for longitudinal absorbed dose and dose equivalent in materials over the energy region of 1 GeV < E_o < 1 TeV. This has been done for the dose on the z- axis (subscripts "a") and for the dose averaged over a 15 cm radius about the z -axis (subscripts "*15* "). Table 2.1 gives parameters for calculating dose equivalent, H_{long} (Sv per electron), at the end of a beam dump of length, L (cm) of density, ρ (g/cm^3), and gives fitted values of the various "attenuation lengths", λ_i (g/cm^2) to be used with the tabulated values of S_i. For absorbed dose calculations, the factor C, which is the ratio of dose equivalent in tissue (Sv) to absorbed dose in the material (not tissue) (Gy), should be set to unity. The formula in which these parameters from Table 2.1 are to be used is as follows:

$$H_{long} = CS_i \exp(-\rho L / \lambda_i). \tag{2.17}$$

This equation is valid in the longitudinal region beyond the shower maximum.

Lateral shower development

Figure 2.6 shows the fraction U/E_o of the incident electron energy which escapes laterally from an infinitely long cylinder as a function of cylinder radius, R, for showers caused by electrons of various energies which bombard the front face of the cylinder. On this graph R is in units of X_m . The curve which fits data between 100 MeV and 20 GeV for electrons incident on targets ranging from aluminum to lead is given by

$$\frac{U(R / X_m)}{E_0} = 0.8\exp[-3.45(R / X_m)] + 0.2\exp[-0.889(R / X_m)]. \tag{2.18}$$

Results similar to this universal curve have been obtained using EGS4 (Sc90). For large values of R/X_m, a material dependent phenomenon emerges in which the photons having the largest mean free paths determined by the photon cross section at the Compton minimum will dominate the slopes of these curves. These slopes, normalized to X_m, are also shown in this figure. As was done for the longitudinal situation, EGS4 (Sc90) has been similarly used to give the maximum energy deposition (and by extension, the maximum absorbed dose and dose equivalent) as a function of radius R. Over the energy range 1 GeV < E_o < 1 TeV, there is direct scaling with energy in the formula for dose equivalent:

$$H_{lat} = CE_0 S_{lat} \frac{\exp(-\rho\, d / \lambda_{lat})}{r^2}, \tag{2.19}$$

where H_{lat} is the maximum dose equivalent laterally (Sv per electron), C is the same as before, E_o is the electron kinetic energy in GeV, S_{lat} is the source term from the EGS4 calculations (see Table 2.2), d is the lateral dimension of the shield (shield thickness) in cm, ρ is the density (g cm^{-3}), λ_{lat} is the attenuation length (g/cm^2), and r is the distance from the axis, in cm, where the dose equivalent is desired (see Fig. 2.3). Table 2.2 gives the parameters needed for Eq (2.19).

Table 2.1 Source terms S_a and S_{15}, and corresponding recommended longitudinal attenuation lengths, λ_a and λ_{15}, for doses on the axis and averaged over a radius of 15 cm in the forward direction for dumps and end-stops. These results are most valid in the region of incident electron energy, E_o, from 1 GeV to 1 TeV. Conversion factors C from absorbed dose in the shielding material to dose equivalent are given. E_o is the beam kinetic energy in GeV. These parameters are to be used with Eq. (2.17). [Adapted from (Sc90).]

Material	C (Sv/Gy)	S_a (Gy/electron)	λ_a (g/cm^2)	S_{15} (Gy/electron)	λ_{15} (g/cm^2)
Water	0.95	$1.9\times10^{-10}E_0^{2.0}$	58	$1.5\times10^{-11}E_0^{2.0}$	59.9
Concrete	1.2	$1.9\times10^{-9}E_0^{1.8}$	44	$2.2\times10^{-11}E_0^{1.8}$	45.6
Aluminum	1.2	$2.3\times10^{-9}E_0^{1.7}$	46	$3.4\times10^{-11}E_0^{1.7}$	46.3
Iron	1.3	$2.9\times10^{-8}E_0^{1.7}$	30	$1.8\times10^{-10}E_0^{1.7}$	33.6
Lead	1.8	$1.9\times10^{-7}E_0^{1.4}$	18	$4.6\times10^{-10}E_0^{1.4}$	24.2

Table 2.2 Conversion factors C from absorbed dose in shielding material to dose equivalent, source terms S_{lat} for the maximum of the electromagnetic component, and recommended lateral attenuation lengths λ_{lat} for the electron energy range, E_o, from 1 GeV to 1 TeV laterally for dumps or end-stops. These parameters are to be used with Eq. (2.19). [Adapted from (Sc90).]

Material	C (Sv/Gy)	S_{lat} (Gy cm^2 GeV^{-1} per electron)	λ_{lat} (g/cm^2)
Water	0.95	2.5×10^{-12}	26
Concrete	1.2	3.6×10^{-12}	27
Aluminum	1.2	3.4×10^{-12}	29
Iron	1.3	4.7×10^{-11}	33
Lead	1.8	1.3×10^{-10}	26

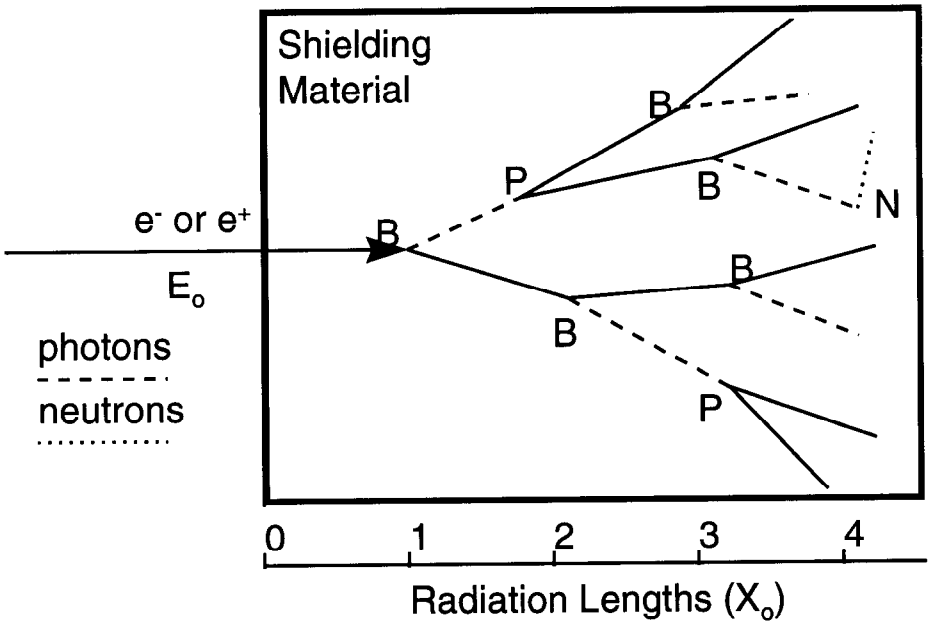

Fig. 2.4 Conceptual view of the development of an electromagnetic cascade in a semi-infinite medium indicated by the shaded area. The solid lines represent electrons or positrons, the dashed lines represent photons, and the dotted lines represent neutrons. The shower is initiated by an electron or positron of energy E_o incident on the medium from the left. The spreading in the transverse direction is greatly exaggerated for clarify. Bremsstrahlung and pair production events are denoted by B and P, respectively. Compton scattering and ionization also play a roles in the dispersal of energy. Photonuclear reactions, as illustrated by the (γ, n) reaction at point N also play a role, albeit much more infrequently than inferred from this illustration. The process could just as well be initiated by a photon. [Adapted from (Sw79).]

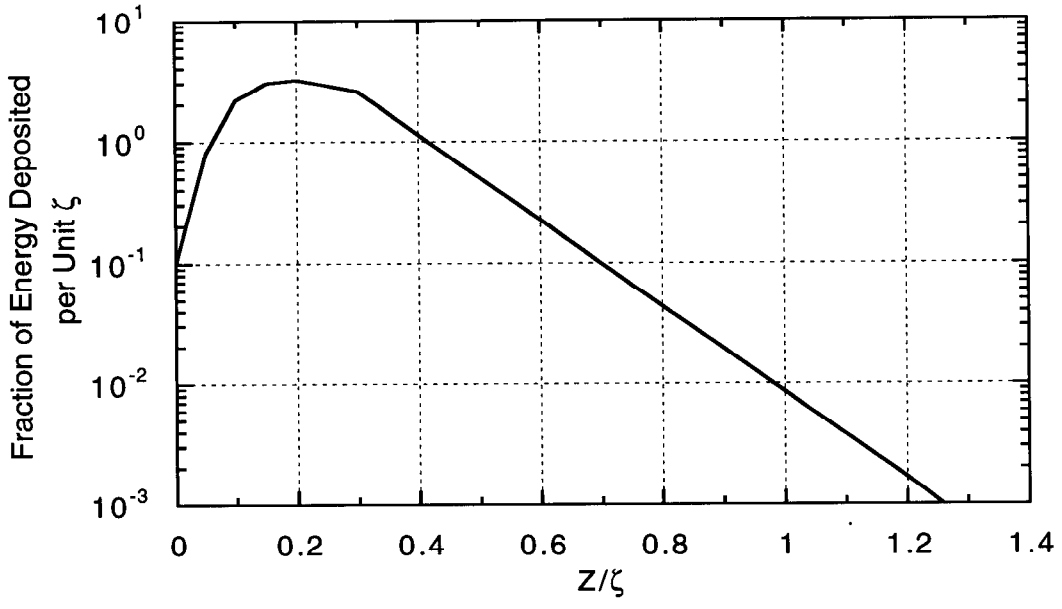

Fig. 2.5 Fraction of total energy deposited by an electromagnetic cascade versus depth integrated over all radii about the shower axis. See Eq. (2.12). [Adapted from (Va75).]

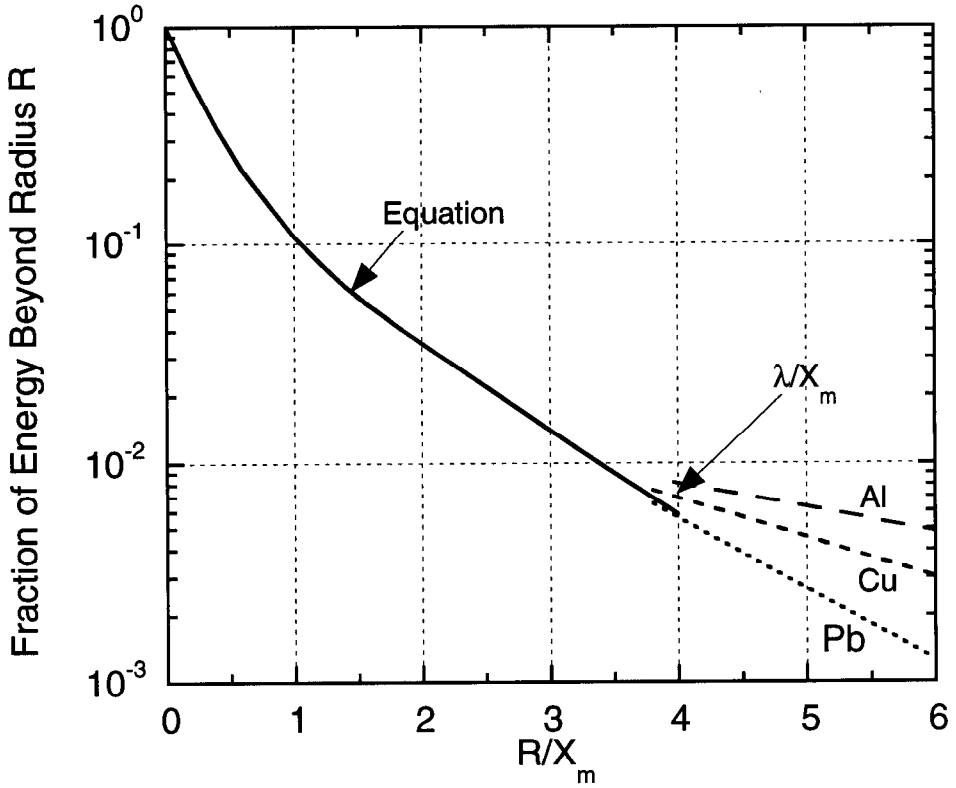

Fig. 2.6 Fraction of total energy deposited beyond a cylindrical radius, R/X_m, as a function of radius, R, for showers caused by 0.1 to 20 GeV electrons incident on various materials. The curve labeled "Equation" refers to Eq. (2.18). [Adapted from (Ne68).]

III. Hadron Production by the Electromagnetic Cascade.

As discussed before, neutrons are produced by high energy electrons and photons. These neutrons must be taken into account to properly shield electron accelerators. Tesch has summarized shielding against these neutrons by developing simple analytical relations for cases where thick targets are struck by the electron beam (Te88). For lateral concrete shielding, the maximum dose equivalent outside of shield thickness, d (cm), which begins at radius a (meters) from an iron target struck by electrons having primary energy E_o (GeV) is, per incident electron,

$$H(d,a) = \frac{4.0\times10^{-17}}{(a+d)^2} E_0 e^{-\rho d/100} \quad \text{(Sv)}. \tag{2.20}$$

This is valid for $E_o > 0.4$ GeV and $\rho d > 200$ g cm^{-2}. The angular variations are not severe because of the nature of the mechanisms by which the neutrons are produced at electron accelerators (namely, photoneutron production). For other target materials one can scale this equation in the following way. The neutron production is proportional to the photoproduction cross section, the track length in cm, and the number of atoms cm^{-3}. The interaction cross section is generally proportional to the atomic weight A. Since the track length is proportional to X_o; the production becomes proportional to the radiation length in units of g cm^{-2}. Thus one can, for rough estimates of dose equivalent in the environs of targets of materials other than iron, obtain results by scaling this value for iron by the factor f;

$$f = \frac{X_0(material)}{X_0(iron)}. \tag{2.21}$$

For shields comprised of other materials, one can simply adjust the attenuation length (g cm^{-2}), i.e., the value of 100 g cm^{-2} in the exponential function, to that appropriate to the material.

Schopper et al. (Sc90) gives a somewhat more detailed treatment separately handling the giant resonance neutrons and high energy particle components of dose equivalent while deriving "source terms" and appropriate formulas. As above, the geometry for using the formulas given here is defined in Fig. 2.3. The formulae given below are held to be valid for 1 GeV $< E_o <$ 1 TeV and for $30 < \theta < 120$ degrees.

For the giant resonance neutrons, per incident electron,

$$H_n = \eta_n S_n E_0 \left(\frac{\sin\theta}{a+d}\right)^2 \exp\left(-\frac{\rho d}{\lambda_n \sin\theta}\right), \quad \text{(Sv)} \tag{2.22}$$

where E_0 is the beam energy (GeV), ρ is the density in g/cm^3, a and d are in cm. S_n is the source term from Table 1.3 (Sv cm^2 GeV^{-1}), and λ_n (g/cm^2) is the attenuation length recommended for giant resonance neutrons. Values of λ_n are given as follows for

representative materials. This formula is regarded as being valid for 30 $< \theta <$ 120 degrees.

	λ_n (g/cm^2)
water	9
concrete	42
iron	130
lead	235.

The factor η_n ($\eta_n \leq 1$) is dimensionless and gives an estimate of the efficiency for the production of neutrons by the target. It smoothly increases from very small values to unity as the target thickness approaches X_o.

For the high energy particles:

In this case no correction for target thickness is generally employed. This formula uses the same source term as Eq (1.36), per incident electron,

$$H_h = \frac{7.5\times10^{-13}\,E_o}{(1-0.75\cos\theta)^2\,A^{0.4}}\left[\frac{\sin\theta}{a+d}\right]^2 \exp\left[-\frac{\rho\,d}{\lambda_h \sin\theta}\right]. \qquad (2.23)$$

In this formula H_h is the dose equivalent due to these particles (Sv), E_o is the beam energy (GeV), A is the atomic weight of the target and λ_h (g/cm^2) is the attenuation length typical of these particles. Table 2.3 gives values of λ_h for representative materials. Schopper et al. (Sc90) goes further and describes a variety of special cases.

Table 2.3 Attenuation lengths λ_h in g/cm^2 for the high energy particle component. [Adapted from (Sc90).]

Material	Energy Limit > 14 MeV or > 25 MeV (g/cm^2)	Energy Limit > 100 MeV	Nuclear Interaction Length (g/cm^2)	Recommended λ_h [Eq. (2.23)] (g/cm^2)
Water			84.9	86
Aluminum			106.4	128
Soil (sand)	101...104*	117	99.2	117
	102...105+	96		
Concrete	101...105*	120	99.9	117
	91	105		
	82...100+	100		
Iron	139+		131.9	164
Lead	244+		194	253

*Attenuation lengths for the indicated values are slightly dependent on angle with the higher value at $\theta = 0^o$ and the smaller value in the backward direction for $E > 15$ MeV.

+Same remark but for $E > 25$ MeV.

IV. Theory of Radiation Transport and the Monte Carlo Method

The theoretical material in this section is largely due to O'Brien (OB80). It is included to show clearly the mathematical basis of the contents of shielding codes, especially those that use the Monte-Carlo method.

General Considerations

Stray and direct radiations at any location are distributed in particle type, direction, and energy. To determine the amount of radiation present for radiation protection purposes we must assign a magnitude to this multidimensional quantity. This is done by forming a double integral over energy and direction of the product of the flux and an approximate flux-to-dose or flux-to-dose-equivalent conversion factor, summed over particle type;

$$H(\vec{x},t) = \sum_i \oint_{4\pi} d\vec{\Omega} \int_0^\infty dE f_i(\vec{x},E,\vec{\Omega},t) P_i(E) \tag{2.24}$$

where the summation index i is over the various particle types, $\vec{\Omega}$ is the direction vector of particle travel, $\vec{x}$ is the coordinate vector of the point in space where the dose or dose equivalent is to be calculated, E is the particle energy, t is time, and i is the particle type. $P_i(E)$ is the dose equivalent per unit fluence conversion factor expressed as a function of energy and particle type. The inner integral is over all energies while the outer integral is over all spatial directions from which contribute to the radiation field at the location specified by $\vec{x}$. The result of the integration is H, the dose or dose-equivalent rate at location $\vec{x}$. Values of $P_i(E)$ are given in Figs. 1.4 and 1.5. The angular flux, $f_i(\vec{x},E,\vec{\Omega},t)$, the number of particles of type i per unit area, per unit energy, per unit solid angle, per unit time at location $\vec{x}$, with a energy E, at a time t and traveling in a direction $\vec{\Omega}$ is related to the flux density, $\phi_i(\vec{x},t)$, by integrating over direction,

$$\phi_i(\vec{x},t) = \oint_{4\pi} d\vec{\Omega} \int_0^\infty dE f_i(\vec{x},E,\vec{\Omega},t), \tag{2.25}$$

to the fluence by integrating over the intervening period of time (t_i to t_f),

$$\Phi_i(\vec{x}) = \oint_{4\pi} d\vec{\Omega} \int_0^\infty dE \int_{t_i}^{t_f} dt f_i(\vec{x},E,\vec{\Omega},t), \tag{2.26}$$

and to the energy spectrum at point $\vec{x}$ at time t by,

$$\phi_i(\vec{x},t,E) = \oint_{4\pi} d\vec{\Omega} f_i(\vec{x},E,\vec{\Omega},t). \tag{2.27}$$

To determine the proper dimensions and composition of a shield, the amount of radiation (expressed in terms of the dose or dose equivalent) which penetrates the shield and reaches locations of interest must be calculated. This quantity must be compared with

the maximum permissible dose equivalent. If the calculated dose equivalent is too large, either the conditions associated with the source of the radiation or the physical properties of the shield must be changed. The latter could be a change in shield materials and/or dimensions. If the shield cannot be adjusted, then the amount of beam loss allowed by the beam control instrumentation, the amount of residual gas in the vacuum system, or the amount of beam accelerated may have to be reduced. It is difficult and expensive, especially in the case of the larger accelerators, to alter permanent shielding or operating conditions if the determination of shielding dimensions and composition has not been done correctly. The methods for determining these quantities have been investigated by numerous workers. The next section only summarizes the basics of this important work.

The Boltzmann Equation

The primary tool for determining the amount of radiation reaching a given location is the Boltzmann equation which, when solved, yields the angular flux, f_i, the distribution in energy and angle for each particle type as a function of position and time. The angular flux is then converted to dose equivalent by means of Eq. (2.24). This section describes the theory that yields the distribution of radiation in matter, and discusses some of the methods for extracting detailed numerical values for elements of this distribution such as particle flux, or related quantities, such as dose, activation or instrument response. The basis for this theory is the stationary form of the Boltzmann equation (henceforth, referred to simply as the Boltzmann equation) which is a statement of all the processes that the corpuscles of various types that comprise the radiation field can undergo.

The Boltzmann equation is an integrodifferential equation describing the behavior of a dilute assemblage of corpuscles. It was derived by Ludwig Boltzmann in 1872 to study the properties of gases but applies equally to the behavior of those "corpuscles" which comprise ionizing radiation. Boltzmann's equation is a continuity equation of the angular flux, f_i, in phase space which is made up of the three space coordinates of Euclidian geometry, the three corresponding direction cosines and the kinetic energy. The density of radiation in a volume of phase space may change in five ways:

1. Uniform translation; where the spatial coordinates change, but the energy-angle coordinates remain unchanged;

2. Collisions; as a result of which the energy-angle coordinates change, but the spatial coordinates remain unchanged, or the particle may be absorbed and disappear altogether;

3. Continuous slowing down; in which uniform translation is combined with continuous energy loss;

4. Decay; where particles are changed through radioactive transmutation into particles of another kind; and

5. Introduction; involving the direct emission of a particle from a source into the volume of phase space of interest: electrons or photons from radioactive materials, neutrons from an α-n emitter, the "appearance" of beam particles, or particles emitted from a collision at another (usually higher) energy.

Combining these five elements yields

$$\mathbf{B}_i f_i(\vec{x},E,\vec{\Omega},t) = Q_{ij} + Y_{ij} \tag{2.28}$$

where the mixed differential and integral *operator,* $\mathbf{B}_i$, is given by

$$\mathbf{B}_i = \vec{\Omega}\cdot\nabla + \sigma_i + d_i - \left\{\frac{\int dE}{\int EdE}\right\}S_i \tag{2.29}$$

$$Q_{ij} = \sum_j \oint_{4\pi} d\vec{\Omega}' \int_o^{E\max} dE_B \sigma_{ij}\left(E_B \rightarrow E,\vec{\Omega}' \rightarrow \vec{\Omega}\right) f_j(\vec{x},E,\vec{\Omega}',t) \tag{2.30}$$

and $$d_i = \frac{\sqrt{1-\beta_i^2}}{\tau_i \beta_i c} \tag{2.31}$$

$\mathbf{B}_i$ is the Boltzmann *operator* for particles of type i;

Y_i is the number of particles of type i introduced by a source per unit area, time, energy, and solid angle;

σ_i is the absorption cross section for particles of type i. To be dimensionally correct, this is actually the macroscopic cross section or linear absorption coefficient $\mu = N\sigma$ as defined in Chapter 1;

d_i is the decay probability per unit flight path of radioactive particles (such as muons or pions) of type i ;

S_i is the stopping power for charged particles of type i (assumed to be zero for uncharged particles);

Q_{ij} is the "scattering-down" integral, the production rate of particles of type i with a direction $\vec{\Omega}$, an energy E at a location $\vec{x}$, by collisions with nuclei or decay of j -type particles having a direction $\vec{\Omega}'$ at a higher energy E_B;

σ_{ij} is the doubly-differential inclusive cross section for the production of type-i particles with energy E and a direction $\vec{\Omega}$ from nuclear collisions or decay of type-j particles with a direction E_B and a direction $\vec{\Omega}'$;

β_i is the velocity of a particle of type i divided by the speed of light c ;
and τ_i is the mean life of a radioactive particle of type i in the rest frame.

This equation is quite difficult to solve in general and special techniques have been devised to yield useful results. The Monte-Carlo method is the most common method of solution used in field of radiation shielding.

The Monte Carlo method-general principles

The Monte Carlo method is based on the use of random sampling to obtain the solution of the Boltzmann equation. It is one of the most useful methods for evaluating radiation hazards for realistic geometries that are generally quite complicated to model using analytic techniques. The calculation proceeds by constructing a series of trajectories, each segment of which is chosen at random from a distribution of applicable processes. In the simplest and most widely used form of the Monte Carlo technique, a history is obtained by calculating travel distances between collisions, then sampling from distributions in energy and angle made up from the cross sections,

$$\sigma_{ij}(E_B \rightarrow E, \vec{\Omega}' \rightarrow \vec{\Omega}) . \tag{2.32}$$

The result of the interaction may be a number of particles of varying types, energies, and directions each of which will be followed in turn. The results of many histories will be processed, leading typically to some sort of mean and standard deviation.

If $p(x)dx$ is the probability of an occurrence at $x \pm 1/2\ dx$ in the interval, $[a,b]$, then

$$P(x) = \int_a^x dx' p(x') \tag{2.33}$$

is the cumulative probability that the event will occur in the interval $[a, x]$, and is monotonically increasing, satisfying $P(a) = 0$, $P(b) = 1$. If a random number R is chosen, uniform on the interval [0, 1] from a computer routine, the equation,

$$R = P(x), \tag{2.34}$$

amounts to a random choice of the value of x, where the distribution function for the event $P(x)$ can be inverted, as

$$x = P^{-1}(R) . \tag{2.35}$$

As a simple illustration, to determine when an uncharged particle undergoes a reaction in a one dimensional system with no decays ($d = 0$) or competing processes ($S = 0$), we note from Eq. (1.6) that the particle satisfies

$$\mathbf{B}_i \phi = \left\{ \vec{\Omega} \cdot \nabla + \sigma_i \right\} \phi \tag{2.36}$$

that in this simple situation reduces to the following, taking in this discussion, σ_t to be the *macroscopic* cross section otherwise denoted by $N\sigma$ in this text.,

$$\mathbf{B}\phi = \frac{d\phi}{dx} + N\sigma\phi = 0 \quad . \tag{2.37}$$

The solution to this equation is the familiar

$$\phi = \phi_0 \exp(-x/\lambda) \ , \tag{2.38}$$

where $\lambda = 1/N\sigma$ as in Chapter 1. One can replace x/λ with r, the number of mean-free-paths the particle travels in the medium. The differential probability per unit mean-free-path for an interaction is given by

$$p(r) = \exp(-r) \tag{2.39}$$

$$\text{with} \quad P(r) = \int_0^r dr' \exp(-r') = -\exp(-r') \Big|_o^r = 1 - \exp(-r) = R \, . \tag{2.40}$$

Selecting a random number, R, then determines a depth r that has the proper distribution. By taking into account charged-particle slowing down during passage along r, the correct energy-dependent cross section can be chosen. Of course, quite analogous methods apply to other processes described by an exponential such as radioactive decay. In this simple case, it is clear that one can solve the above for r as a function of R and thus obtain individual values of r from random numbers. For most process, the inversion that is so simple in the above might not be possible analytically. In those situations, other techniques exemplified by successive approximation and "table look-ups" must be employed.

The next sampling process might select which of several physical processes would occur. Another sampling might choose, for instance, the scattering. Deflections by magnetic fields might be included as well as further particle production and/or decay.

The Monte Carlo result is the number of times the event of interest occurred for the random steps through the relevant processes. As a counting process it has a counting uncertainty and the variance will tend to decrease as the square root of the number of calculations run on the computer. Thus high probability processes can be more accurately estimated than low probability processes such as passage through an effective shield in which the radiation levels are attenuated over many orders of magnitude. Sophisticated techniques are employed which temporarily give enhanced probabilities to the low-probability events during the calculation in order to study them with the normal probabilities restored at the end of the calculation by removing these so-called "weights". It is by no means clear that the distributions obtained using the Monte Carlo method will be normally distributed, so that a statistical test of the adequacy of the mean and standard deviation may be required.

Monte-Carlo Example; A Sinusoidal Angular Distribution of Beam Particles

Suppose one has a distribution of beam particle particles such as exhibited in Fig 2.7. For this distribution, $p(\theta) = A \cos\theta$ for $0 < \theta < \pi/2$. Then, the fact that the integral of $p(\theta)$ over the relevant interval must be unity implies $A = 1$ since

$$P(\pi/2) = \int_0^{\pi/2} d\theta A \cos\theta = A \sin\theta \Big|_0^{\pi/2} \overset{\text{def}}{=} 1. \tag{2.41}$$

Then, $p(\theta) = \cos\theta$. The cumulative probability, $P(\theta)$, is given by:

$$P(\theta) = \int_o^{\theta} d\theta' p(\theta') = \int_o^{\theta} d\theta' \cos\theta' = \sin\theta' \Big|_o^{\theta} = \sin\theta \tag{2.42}$$

If R is a random number, then $R = P(\theta)$ determines a unique value of θ; hence:

$$\theta = \sin^{-1}(R). \tag{2.43}$$

One can perform a simple Monte Carlo calculation using, for example, 50 random numbers. To do this one should set up at table such as that given below which was generated using a particular set of such random numbers. One can set up a set of bins of succesive ranges of θ-values. The second column is a "tally sheet" for collecting "events" in which a random number R results in a value of θ within the associated range of θ-values. θ_{mid} is the midpoint of the bin (0.1, 0.3,...). Column 4 is the normalized number in radians found from:

$$N = \frac{\text{Number found in Monte Carlo bin}}{(\text{Total number of events})(\text{bin width})} = \frac{\text{Number found in bin in Monte Carlo}}{(50)(0.2 \text{ radians})} \tag{2.44}$$

θ (radians)	R (random #)	Total R's in Bin	N (norm. #)	cos θ_{mid}
0.0 - 0.199	~~1111~~ ~~1111~~ 1	11	1.1	0.995
0.2 - 0.399	~~1111~~ ~~1111~~111	13	1.3	0.955
0.4 - 0.599	~~1111~~ ~~1111~~ 1	11	1.1	0.877
0.6 - 0.799	1111	4	0.4	0.765
0.8 - 0.999	~~1111~~ 11	7	0.7	0.621
1.0 - 1.199	1111	4	0.4	0.453
1.2 - 1.399				0.267
1.4 - 1.57				0.086

One can calculate exactly the mean value of θ for the specified distribution:

$$\langle\theta\rangle = \frac{\int_0^{\pi/2} \theta p(\theta) d\theta}{\int_0^{\pi/2} p(\theta) d\theta} = \frac{\int_0^{\pi/2} \theta \cos\theta d\theta}{1} = [\cos\theta + \theta \sin\theta]_0^{\pi/2}$$

$$\langle\theta\rangle = \left[0 - 1 + \frac{\pi}{2} - 0\right] = 0.57 \qquad (2.45)$$

By multiplying the frequency of Monte-Carlo events for each eight angular bins from the table by the midpoint value of the bins, summing over the 8 bins and then dividing by the number of incident particles (50 in this example), one can determine the average value of θ, $<\theta>_{MC}$ calculated by the Monte-Carlo technique:

$$<\theta>_{MC} = [(11)(0.1) + (13)(0.3) + (11)(0.5) + (4)(0.7) + (7)(0.9) + (4)(1.1)]/50 = 0.48.$$

It is easy to see from this simple example that the agreement is quite good in spite of the rather poor "statistics". This example also illustrates that the statistical errors are generally larger for the more rare events here represented by large values of θ (i.e., $\theta > 1$ radian).

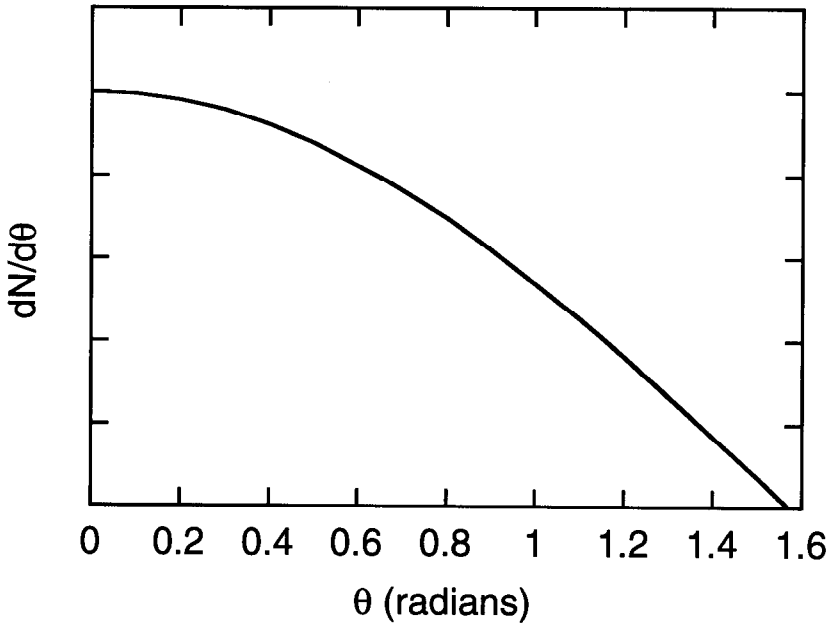

Fig. 2.7 Hypothetical angular distribution of particle obeying a distribution proportional to the cos θ.

V. Brief Review of Magnetic Deflection of Charged Particles

Particle accelerators of all types operate by utilizing electromagnetic forces to accelerate and deflect charged particles. These forces have been well described in detail by other authors such as Edwards and Syphers (Ed93) and Carey (Ca87). The forces are encountered in accelerator radiation protection most prominently by the need to determine if a given deflection by an electric or magnetic field is sufficient to assure that a particle beam either interacts with material where such interactions are desired or avoids such points of beam loss. The answers to such questions can become interconnected with the design of the accelerator and for those purposes, advanced texts such as those cited above should be consulted. This is especially true for situations involving the application of radiofrequency waves to the particle beams where a full treatment using electrodynamics is needed. However, some of the issues are quite simple.

The force, $\vec{F}$ (newtons) on a given charge, q (Coulombs), at any point in space is given, in SI units, by

$$\vec{F} = q(\vec{v} \times \vec{B} + \vec{E}) = \frac{d\vec{p}}{dt}, \tag{2.46}$$

where the electric field, $\vec{E}$, is in volts/meter, and the magnetic field $\vec{B}$ is in Tesla (1 Tesla = 10^4 Gauss). As always, $\vec{p}$ is the momentum of the particle in SI units, and t is the time. The direction of the force due to the cross product in Eq (2.46) is, of course, determined by the usual "right-hand" rule. Application of static, uniform electric fields simply serve to accelerate or decelerate the charged particles. In a uniform magnetic field without the presence of an electric field, due to the cross product in this equation, any component of $\vec{p}$ which is parallel to $\vec{B}$ will not be altered by the magnetic field. Thus, one is only concerned with the component of $\vec{p}$ which is perpendicular to $\vec{B}$. Typically, charged particles are deflected by dipole magnets in which the magnetic field is, to high order, "uniform" and constant in time, or slowly varying compared with the time during which the particle is present. For this situation, if there is no component of $\vec{p}$ which is parallel to $\vec{B}$, the motion is circular and the magnetic force serves to supply the requisite centripetal acceleration. The presence of a component of $\vec{p}$ which is parallel to $\vec{B}$ results in a trajectory which is a spiral rather than a circle. Figure 2.8 illustrates the condition of circular motion. Equating the centripetal force to the magnetic force leads to,

$$\frac{mv^2}{R} = qvB, \tag{2.47}$$

where m is be the *relativistic* mass (see Eq. 1.11). Solving for the radius of the circle, R (meters), and recognizing that $p=mv$, one gets,

$$R(\text{meters}) = \frac{p}{qB}\ (\text{mks units}) = \frac{p(\text{GeV}/c)}{0.29979qB(\text{Tesla})}, \tag{2.48}$$

where q in the denominator is now the *number* of electronic charges carried by the particle. The numerical factor in the denominator is just the mantissa of the numerical value of the speed of light in SI units. In practice, at large accelerators, one is often interested in the angular deflection of a magnet of length, L, which provides such a uniform field orthogonal to the particle trajectory. Such a situation is also shown in Fig. 2.8. If L is only a small piece of the complete circle (i.e., L << R), one can consider the circular path over such a length to be a straight line segment. Doing this, one finds that the change in direction, $\Delta\theta$, is given by

$$\Delta\theta = \frac{L}{R} = \frac{0.29979qBL}{p}\ (\text{radians}), \tag{2.49}$$

where the product, BL (Tesla-meters) is commonly referred to the **field integral** of the magnet system and p is in GeV/c. It is evident that BL could just as well be obtained by integrating a non-uniform field over the length of the magnet system. This angle of deflection can be used to deduce if the particle beam will, or will not, interact with some solid object near its path. Edwards and Syphers (Ed93) and Carey (Ca87) go further to describe the magnetic deflections provided by more general electromagnetic systems, including the effects of quadrupole magnets, and those of higher order which focus particle beams. Mathematical methods analogous to those found in the study of geometric optics are often used to describe the optics of charged particles. Where time-varying electric and magnetic fields are involved, the full complement of Maxwell's equations must, of course, be used to describe the motion of charged particles.

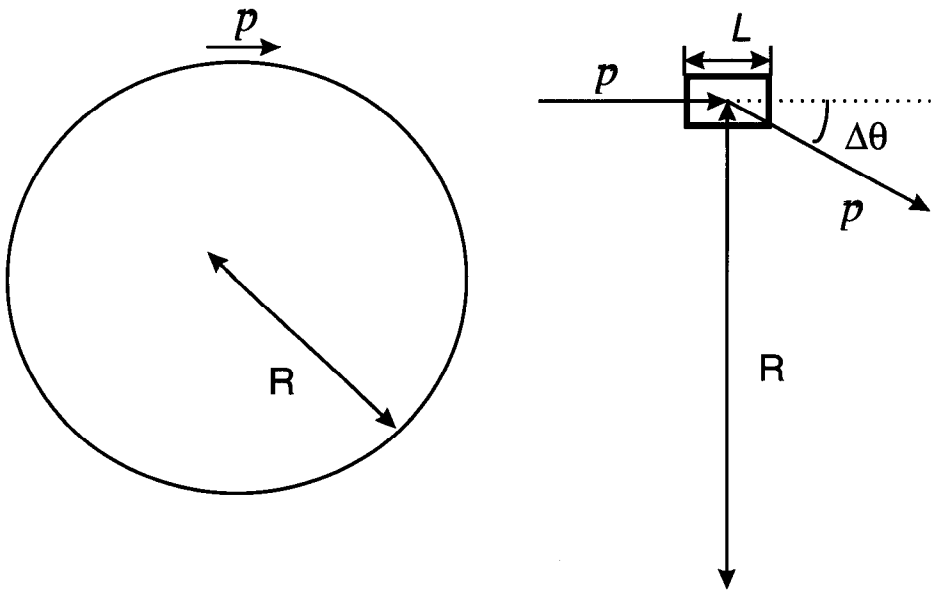

B is perpendicular to the paper and directed toward the reader

Fig. 2.8 A particle of charge q having momentum p follows a circular path when directed perpendicular to a static uniform magnetic field. The figure on the left illustrates this for a complete circle. On the right, a particle of such momentum enters a magnet of length L that has field integral value of BL. In this situation, $L<<R$ and the particle experiences a small angular deflection $\Delta\theta$. The angular deflection is exaggerated in this figure for clarity.

References

(Ba67) G. Barthow, E. Freytag, and K. Tesch, "Measurements on 6.3 GeV electromagnetic cascades and cascade producing neutrons", Nucl. Phys. B2 (1967) 669-689.

(Ca87) D. C. Carey, *The optics of charged particle beams* (Harwood Academic Publishers, New York 1987).

(Ed93) D. A. Edwards and M. J. Syphers, *An introduction to the physics of high energy accelerators* (John Wiley and Sons, Inc., New York, 1993).

(IC87) International Commission on Radiological Protection, "Data for use in protection against external radiation, ICRP Report No. 51 (1987).

(Ne68) R. B. Neal, editor, *The Stanford two mile accelerator* (Benjamin, New York, 1968).

(Ne90) W. R. Nelson, H. Hirayama, and D. W. O. Rogers, "The EGS4 code system", SLAC-265, Stanford Linear Accelerator Center (December, 1985). [EGS4 has been thoroughly reviewed in Kase, Bjarngard, and Attix, in *The Dosimetry of ionizing radiation,* Volume III (Academic Press, 1990)]

(Ne97) W. R. Nelson, private communication, 1997.

(OB80) K. O'Brien, "The physics of radiation transport" in *Computer techniques in radiation transport dosimetry*, W. R. Nelson and T. M. Jenkins, Editors, Ettore Majorana International Science Series (Plenum Press, New York, 1978), pp. 17-56.

(PDG96) Particle Data Group, *Review of particle properties,* Physical Review D54, Part I (July, 1996).

(Ro41) B. Rossi and K. Greisen, "Cosmic-ray theory", Rev. Mod. Phys., 13 (1941) 240-309. See also B. Rossi, *High energy particles* (Prentice-Hall, Englewood Cliffs, New Jersey, 1952).

(Sc90) H. Schopper (editor), A. Fassò, K. Goebel, M. Höfert, J, Ranft, and G. Stevenson, *Landolt-Börnstein numerical data and runctional relationships in science and technology new series; Group I: Nuclear and particle physics Volume II: Shielding against high energy radiation* (O. Madelung, Editor in Chief, Springer-Verlag, Berlin, Heidelberg, 1990).

(Sw79) W. P. Swanson, "Radiological safety aspects of the operation of electron linear accelerators," Technical Report No. 188, Vienna, 1979.

(Sw90) W. P. Swanson and R. H. Thomas, "Dosimetry for radiological protection at high energy particle accelerators", Chapter 1 in *The Dosimetry of ionizing radiation,* Volume III (Academic Press, 1990).

(Te88) K. Tesch, "Shielding against high energy neutrons from electron accelerators-a review", Rad. Prot. and Dos. 22 (1988) 27-32.

(Va75) A. Van Ginneken and M. Awschalom, "High energy particle interactions in large targets", Vol. 1, Fermi National Accelerator Laboratory Report (1975).

(Va78) A. Van Ginneken, "AEGIS, a program to calculate the average behavior of electromagnetic showers", Fermilab Report FN-309 (1978).

Problems

1. In the discussion of the longitudinal development of electromagnetic showers, there are two different formulations (Rossi-Griesen and Bathow, and Van Ginneken). Using Van Ginneken's scaling method, calculate the value of ζ (g/cm^2) for E_0 = 1000 MeV, 10 GeV, and 100 GeV for copper and lead. Determine the number of radiation lengths to which ζ, corresponds for each material at each energy.

2. Compare the results of Van Ginneken for the location of the longitudinal shower maximum with Bathow's result for copper and lead at the three energies given in problem 1. Is the agreement better or worse as the energy increases?

3. A hypothetical electron accelerator operates at either 100 MeV or 10 GeV and delivers a beam current of 1 μA. Using Table 2.1, calculate the dose equivalent rates in both Sv/sec and rem/h at the end of a 300 cm long aluminum beam stop; averaged over a 15 cm radius that are due to bremsstrahlung. (The beam stop is a cylinder much larger than 15 cm in radius.) Then assume that, in order to save space, a high-*Z* beam stop is substituted. How long of a high-*Z* beam stop is needed to achieve the same dose rates? (Assume lead is a suitable high-*Z* material.) Why is the length of high-*Z* shield different for the 2 energies? In this problem, assume the values in Table 2.1 are valid for energies as low as 0.1 GeV.

4. In the accelerator and beam stop of problem 3, if the radius of the beam stop is 30 cm, what is the maximum dose equivalent rate (Sv/s and rem/h) on the lateral surface (at contact at r = 30 cm) of the beam stop for both energies, 100 MeV and 10 GeV, and both materials? Again assume approximate validity at 100 MeV of the results.

5. Calculate the dose equivalent rate outside a 1 meter thick concrete shield surrounding a cylindrical tunnel (inner radius 1 meter) in which is located a copper target stuck by 1 μA beam of 100 GeV electrons. The geometry should be assumed to be optimized for producing giant resonance photoneutrons and the calculations should be performed at θ = 30, 60 and 90° (Concrete has ρ = 2.5 g/cm^3). Express the result as Sv/sec and rem/h.

6. This problem gives two elementary examples of Monte Carlo techniques that are almost "trivial". In this problem, obtaining random numbers from a standard table or from a hand calculator should be helpful.

   a) First, use a random number table or random number function on a calculator along with the facts given about the cumulative probability distribution for exponential attenuation to demonstrate that, even for a sample size as small as, say, 15, the mean value of paths traveled is "within expectations" if random numbers are used to select those path lengths from the cumulative distribution. Do this, for example, by calculating the mean and standard deviation of your distribution.

   b) An incident beam is subjected to a position measurement in the coordinate x. It is desirable to "recreate" incident beam particles for a shielding study using Monte-Carlo. The x distribution as measured is as follows:

x	#
0	0
1	1
2	2
3	3
4	4
5	5
6	4
7	3
8	2
9	1
10	0

   Determine, crudely, $p(x)$, $P(x)$ and then use 50 random numbers to "create" particles intended to represent this distribution. Then compare with the original one which was measured in terms of the average value of x and its standard deviation. Do <u>not</u> take the time to use interpolated values of x, simply round off to integer values of x for this demonstration.

7. A beam of protons having a kinetic energy of 100 GeV is traveling down a beam line. The beam is entirely contained within a circle of diameter 1 cm. All of the beam particles have the same kinetic energy. An enclosure further downstream must be protected from the beam or secondary particles produced by the beam by shielding it with a large diameter iron block that is 20 cm in radius centered on the beam line. The beam passes by this block by being deflected by a uniform field magnet that is 3 meters long and is located 30 meters upstream of the iron block. Calculate the magnetic field, B, that is needed to accomplish this objective.